

Isotactic polypropylenes of different molecular characteristics: influence of crystallization conditions and annealing on the fracture behaviour

ROBERTO GRECO, GIUSEPPE RAGOSTA

Istituto di Ricerche su Tecnologia dei Polimeri e Reologia del CNR, Via Toiano 6, Arco Felice, Napoli, Italy

Fracture mechanics analysis at high speed and low temperature has been carried out on polypropylene samples of various molecular weights, obtained under different crystallization conditions. In addition differential scanning calorimetry measurements and morphological observations by scanning electron microscopy have been also performed. It has been found that the fracture mechanics parameters G_c and K_c increase markedly with enhancing the molecular weight, whereas an opposite trend is observed with increasing the crystallization temperature. Furthermore it has been seen that an annealing procedure, on the already solidified samples, strongly enhances the fracture toughness parameters. The above findings have been confirmed by fracture surface observations showing that crazing is the dominant feature of deformation in such materials. Possible underlying molecular mechanisms, which can explain the overall properties and the morphological characteristics, are discussed as well.

1. Introduction

The properties of semicrystalline polymers have been extensively investigated in the past several years [1-4]. It is now well established that spherulitic microstructure has a strong influence in determining the fracture behaviour and other physico-mechanical characteristics of such materials [5-9]. However, there is not a complete explanation of the mechanisms through which the various structural elements forming the spherulites control the growth and propagation of cracks in semicrystalline polymers. One aspect that has become increasingly evident over the years is the role of tie-molecules. Electron spin resonance and other studies [10, 11] have showed that these molecules act as local transducers of stress among crystallites and are broken during deformation and fracture. Therefore the number of tie-chains, which is related to the crystallization conditions, can have strong effects on the mechanical and fracture behaviour, even though other structural features developed within spherulites can contribute.

In the present paper the approach of linear elastic fracture mechanics has been used to study the influ-

ence of molecular weight and different heat treatments, such as crystallization conditions and annealing, on the high-speed fracture toughness of polypropylene samples. The aim has been to correlate the fracture mechanics parameters like the critical strain energy release rate (G_c) and the critical stress intensity factor (K_c) with the different microstructures obtained. This should provide also useful information on how the complex spherulitic architecture affects the failure mechanisms. For such a purpose morphological and fractographic analyses by means of scanning electron microscopy (SEM) have also been performed.

2. Experimental procedure

2.1. Materials

Four samples of isotactic polypropylene (PP) with different molar masses and molar mass distributions were used in the present work. Their molecular characteristics, together with their code numbers and sources, are reported in Table 1.

2.2. Specimen preparation

The polymer in chips was placed between two teflon

TABLE I Molecular characteristics of polypropylene samples

Code	Company and trade name	\bar{M}_w	\bar{M}_n	\bar{M}_w/\bar{M}_n
PP1	RAPRA*	3.1×10^5	1.6×10^4	20
PP2	Exxon Chemical Co. PPM 260	4.4×10^5	1.0×10^4	4.4
PP3	Exxon Chemical Co. PPE 111	6.3×10^5	1.9×10^4	3.3
PP4	Montedipe-Himont	8.9×10^5	1.1×10^4	8.2

*Rubber and Plastics Research Association of Great Britain.

TABLE II Crystallization temperatures (T_b) and times (t)

T_b ($^{\circ}\text{C}$)	135	120	90	60	20
t (min)	300	120	30	30	30

sheets and laterally contained in a 4.0 mm thick steel frame. The whole system was inserted within the plates of a hydraulic press heated at 200°C under a pressure of 200 kg cm^{-2} . After a delay of 10 min after melting the pressure was released and the sandwiched sample was suddenly immersed in a glycerol bath and kept at a fixed temperature for certain times.

The temperature of bath (T_b) and the residence times were varied as reported in Table II. Successively the crystallized samples were fast-cooled in ice and water at about 0°C . Some of them were also annealed in a oven at 140°C under vacuum for 24 h. From such sheets rectangular-type specimens ($60\text{ mm} \times 6.0\text{ mm} \times 4.0\text{ mm}$) were cut by means of a saw to obtain samples for impact tests.

Prior to testing the specimens were notched as follows: first a blunt notch was produced using a machine with a V-shaped tool and then a sharp notch 0.2 mm deep was made by a razor fixed to a micrometric apparatus. The final value of the notch depth was measured after fracture by using an optical microscope.

2.3. Thermal analysis

Differential scanning calorimetry measurements to detect melting points (T_m) and crystallinity contents (X_c) were made by a Mettler TA 3000 system apparatus. All the measurements on samples (whose weights ranged from 4.0 to 8.0 mg) were performed at a scanning rate of $20^{\circ}\text{C min}^{-1}$.

2.4. Morphological analysis

Microtomed surfaces were examined by means of a Philips 501 scanning electron microscope. Before observation the specimens were etched with CrO_3 - H_2SO_4 saturated solution to destroy amorphous material among and within spherulites. The etching solution was prepared as follows: first concentrated sulphuric acid (95% by weight) was diluted with water (the ratio of H_2SO_4 to water was 1:4). Then it was heated to about 80°C and the CrO_3 was added to form the saturated solution. Specimens were immersed in the solution for 60 min at 80°C and were then washed with clear water and dried in a vacuum oven for 8 h at 50°C .

2.5. Impact fracture measurements

Fracture tests were carried out on a Charpy instrumented pendulum (Ceast Autographic Pendulum MK2) at an impact speed of 1 m sec^{-1} . Samples with a notch depth-to-width ratio of 0.3 and a span test of 48 mm were fractured at -100°C using liquid nitrogen as a cooling medium. The relevant curves of energy and load against time or displacement were recorded.

2.6. Fracture toughness parameters

The impact data were analysed according to the linear elastic fracture mechanics approach [12]. The critical stress intensity factor K_c , was calculated by means of the equation

$$K_c = \sigma y a^{1/2} \quad (1)$$

where σ is the nominal stress at the onset of crack propagation; a is the initial crack length and Y a calibration factor depending on the specimen geometry. For singly cracked bent specimens, Y is given by Brown and Strawley [13].

For the determination of the critical strain energy release rate G_c , the following equation was used:

$$G_c = U/BW\Phi \quad (2)$$

where U is the fracture energy corrected for the kinetic energy contribution; B and W are the thickness and the width of the specimen, respectively, and Φ is a calibration factor which depends on the length of crack and the size of the sample. The values of Φ were taken from Plati and Williams [14].

2.7. Fractography

Fracture surfaces of notched specimens were examined by SEM, after coating the broken surfaces with a thin layer of gold-palladium alloy.

3. Results and discussion

3.1. Thermal properties

In Table III, the melting points (T_m) and the crystallinity content (X_c) for unannealed and annealed samples are reported as a function of the crystallization temperature T_b .

As shown for unannealed samples, the melting points are scarcely affected by the thermal history and molecular characteristics of PP. Only at high T_b is a slight enhancement in the T_m values observed. This effect seems to be due to the great molecular mobility of the chains and to the long crystallization times.

TABLE III Crystallization temperature (T_b), crystallinity (X_c) and melting temperature (T_m) of annealed and unannealed polypropylene samples

T_b ($^{\circ}\text{C}$)	PP1		PP2				PP3				PP4					
	Annealed		Unannealed		Annealed		Unannealed		Annealed		Unannealed		Annealed		Unannealed	
	X_c	T_m ($^{\circ}\text{C}$)	X_c	T_m ($^{\circ}\text{C}$)	X_c	T_m ($^{\circ}\text{C}$)	X_c	T_m ($^{\circ}\text{C}$)	X_c	T_m ($^{\circ}\text{C}$)	X_c	T_m ($^{\circ}\text{C}$)	X_c	T_m ($^{\circ}\text{C}$)	X_c	T_m ($^{\circ}\text{C}$)
135	59.0	169	58.0	169	56.0	168	53.0	166	54.0	167	53.0	166	50.0	167	48.0	166
120	56.0	168	55.0	167	54.0	166	53.0	165	52.0	165	50.0	165	49.0	165	47.0	165
90	53.0	165	51.0	165	52.0	165	49.0	165	51.0	165	47.0	163	48.0	164	45.0	164
60	52.0	165	49.0	165	50.0	165	47.0	165	49.0	165	46.0	164	47.0	164	43.0	163
20	50.0	165	46.0	165	49.0	165	45.0	165	48.0	164	44.0	163	46.0	164	42.0	162

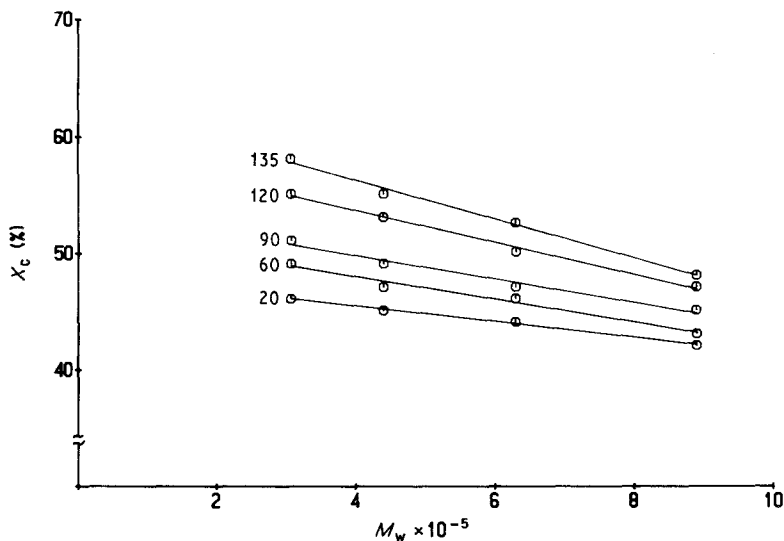


Figure 1 Crystallinity content X_c of unannealed PP samples as a function of molecular weight M_w . Crystallization temperature T_b as indicated.

Such conditions favour the formation of more perfect crystallites, yielding therefore higher T_m values. On the other hand the degree of crystallinity seems to be influenced by the molecular weight (M_w) and crystallization conditions. This dependence, a decreasing linear trend at constant T_b is better seen in Fig. 1 where X_c is plotted as a function of M_w for all the T_b values investigated. As the molecular weight increases the plateau relaxation time, due to chain entanglements, is enhanced and the crystallization occurs locally in a more and more disordered way. Hence the amount of developed crystallinity tends to decrease. On the other hand, at a fixed M_w , the degree of crystallinity increases with increasing T_b , since the crystallization rate is lowered. This renders the polymer chains more mobile and therefore more able to be orderly crystallized. There is a superposed influence of T_b and M_w and therefore the effect is the larger the lower is the molecular weight.

A similar behaviour is observed for annealed samples as reported in Fig. 2. It should be underlined, however, that annealing promotes in all the samples an enhancement of the crystallinity levels compared with the unannealed ones. This result is a consequence of the fact that during such a process further crystallizations take place, mainly in the interspherulitic regions.

3.2. Morphological analysis

Scanning electron micrographs of microtomed and etched surfaces of some of the samples examined are shown in Figs 3 and 4. It can be seen from these figures that the overall morphology is dependent on both the crystallization temperature and the molecular structure of the polypropylene used. Fig. 3 shows the effect of different undercoolings on the dimensions, structure and perfection of spherulites for unannealed PP1 samples. At the crystallization temperature of 135°C (Fig. 3a), large spherulites with open boundaries are visible. In addition adjacent spherulites are bridged only by very few interspherulitic links. This poor interconnection derives from the very slow crystallization rate used to obtain such a morphology. In fact, during the crystallization process, impurities, defective and non-crystallizable molecules can be rejected from the growing fronts of the spherulites. At the end such material, collected in the interspherulitic boundaries, is easily etched out.

Conversely as the crystallization temperature is lowered (Figs 3b to e), the size of the spherulites decreases and the material become more and more compact, since the degree of connection between crystallites and spherulites increases. This is due to the fact that at lower T_b , the nucleation rate and density as well as the overall crystallization rate increase.

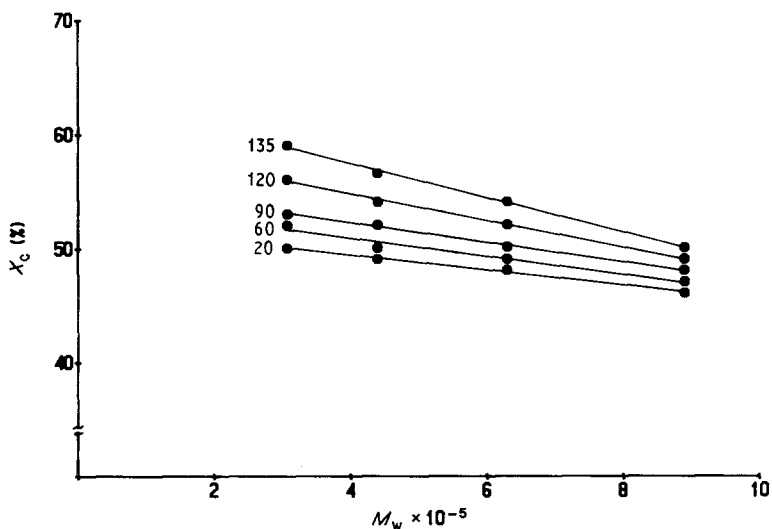


Figure 2 Crystallinity content X_c of annealed PP samples as a function of molecular weight M_w . Crystallization temperature T_b as indicated.

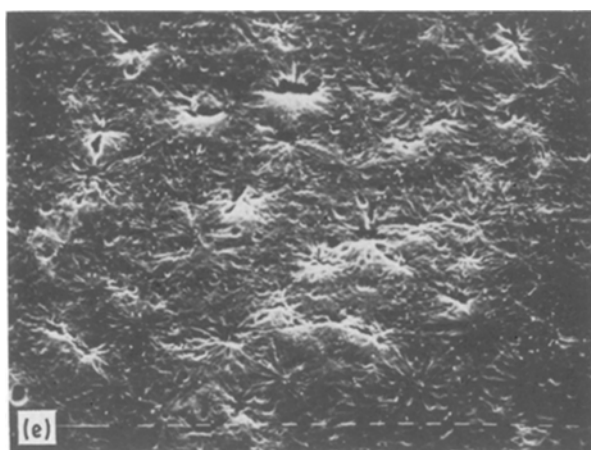
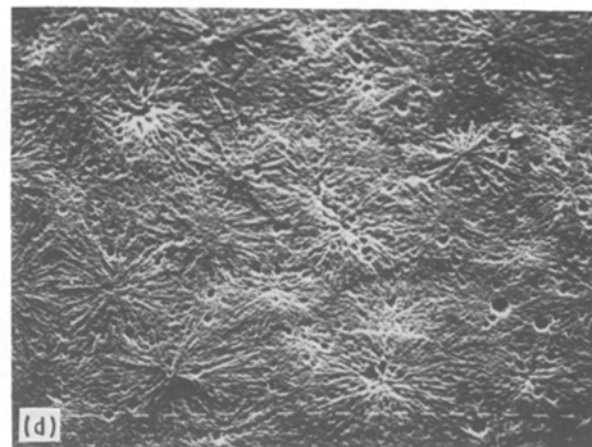
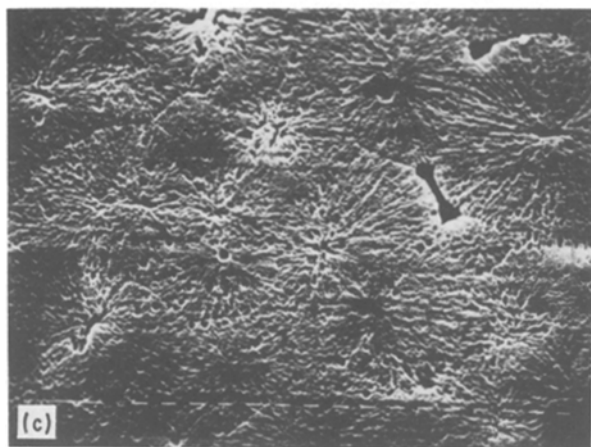
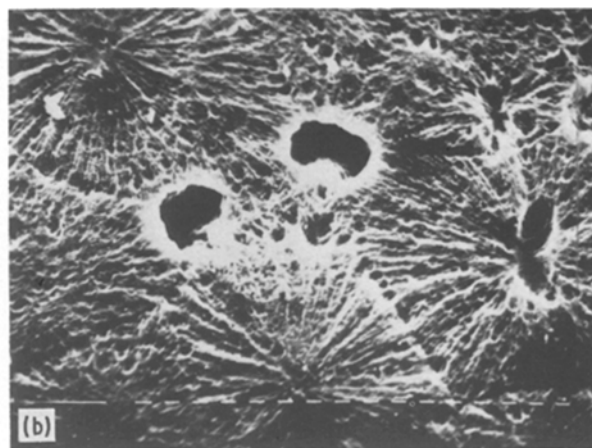
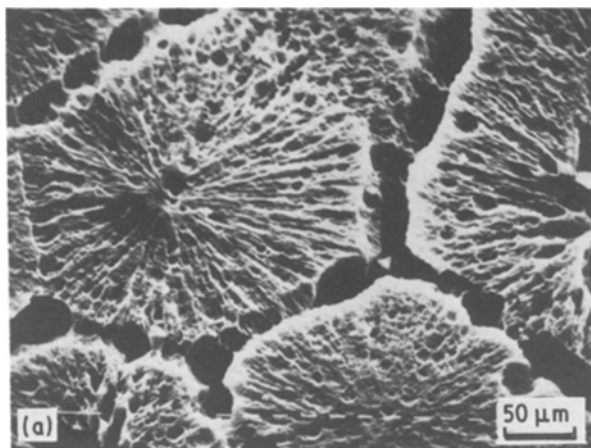


Figure 3 Scanning electron micrographs of smoothed and etched surfaces of unannealed PP1 sample for different crystallization temperatures (T_b): (a) 135°C, (b) 120°C, (c) 90°C, (d) 60°C, (e) 20°C.

This effect tends to freeze somewhat the melt conformations of the molecules, allowing only for local crystallite formation.

This process provides in the fully crystallized sample a number of tie-chains among crystallites which is higher the lower is T_b . The concentration of such tie-chains can also be varied by changing the molecular weight. This is evident in Fig. 4. It shows that under the same crystallization conditions the degree of interconnection within the material increases with enhancing the molecular weight. The higher the molecular weight the longer the polymer chains, and the relative relaxation times. This yields an increased number of tie molecules. Therefore increasing molecular weight has an effect on the tie-chains density similar to that of an increased undercooling. The influ-

ence that these tie-chains have on the crack growth and on the fracture toughness of such materials is reported and discussed in the next section.

3.3. Impact fracture toughness and fractographic analysis

The critical strain energy release rate G_c and the critical stress intensity factor K_c , calculated according to Equations 1 and 2, are reported as a function of the molecular weight M_w in Figs 5 and 6 for unannealed samples and in Figs 7 and 8 for annealed ones.

From these kinds of plots it is possible to make the following observations:

(i) For unannealed samples (Figs 5 and 6), G_c and K_c increase with increasing molecular weight in all the range of T_b investigated. Moreover, for a fixed M_w , decreases in the K_c and G_c values are detected with increasing T_b . This effect is more marked for the lowest M_w sample, probably due to its broad molar mass distribution.

(ii) For annealed materials (Figs 7 and 8) the trend is quite similar, but the values of G_c and K_c are much higher than for the corresponding unannealed materials. Only at $T_b = 135^\circ\text{C}$ with the exception of the highest M_w do the two sets of samples yield identical toughness values.

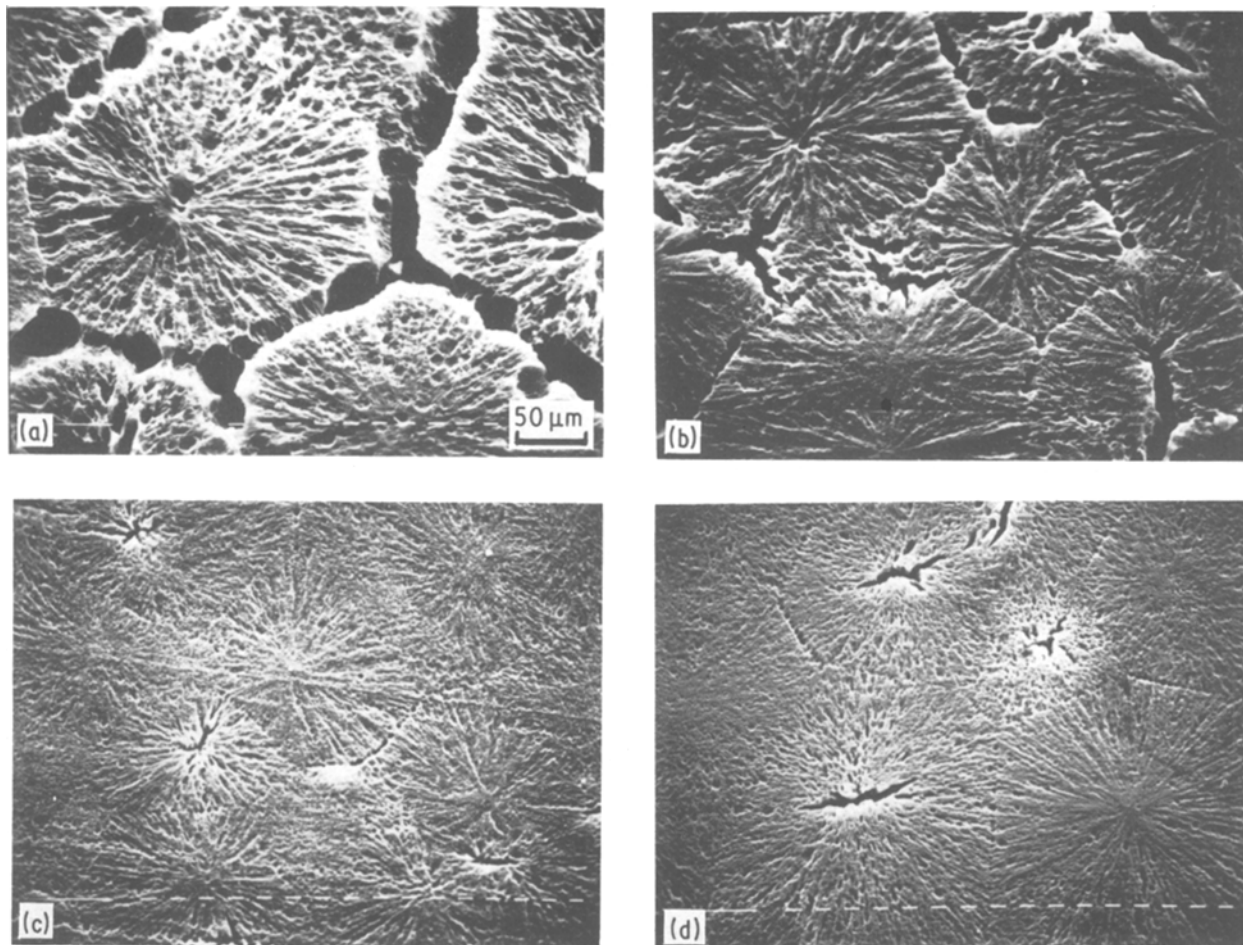


Figure 4 Scanning electron micrographs of smoothed and etched surfaces of unannealed PP samples for different molecular weight and $T_b = 135^\circ\text{C}$. (a) PP1, (b) PP2, (c) PP3, (d) PP4.

On the basis of the above results it emerges that the fracture parameters G_c and K_c of bulk-crystallized polypropylene are particularly suitable to monitor morphological and structural changes induced by different heat treatments and molecular weights. Therefore an attempt was made to correlate such parameters with the resistance offered to crack growth by the various structured elements present in the material such as spherulites and spherulite boundaries. For this purpose two limiting cases were examined, samples crystallized at low and at high T_b .

In Fig. 9 are reported the scanning electron micrographs of fractured surfaces taken near the notch tip of unannealed PP1 samples. As can be seen, the coarse spherulitic material (Fig. 9a) shows a very small amount of plastic deformation in the boundary zones and the spherulites are practically undeformed. Such features are related to the fact that spherulitic boundaries are much less crack-resistant than the inner zones because of the sparsity of interspherulitic links (see Fig. 3a). Therefore they can act as effective crack sites and easy fracture paths. Thus the contribution to the

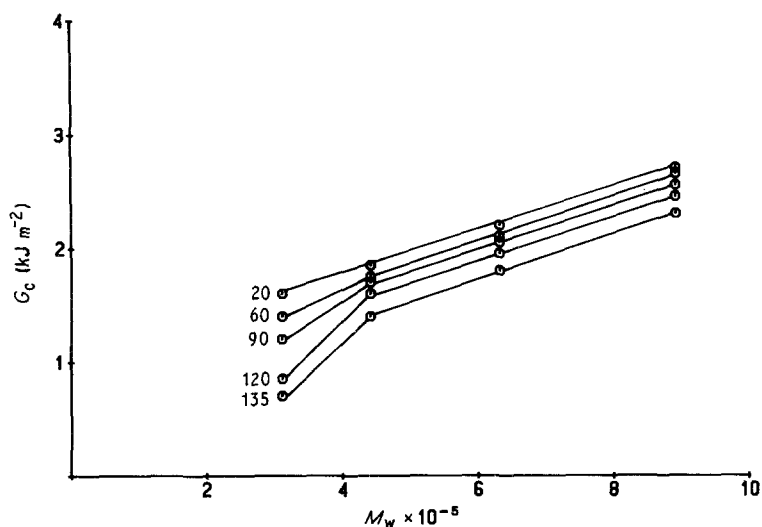


Figure 5 Critical strain energy release rate G_c as a function of molecular weight M_w , for unannealed PP samples crystallized at different temperatures T_b as indicated.

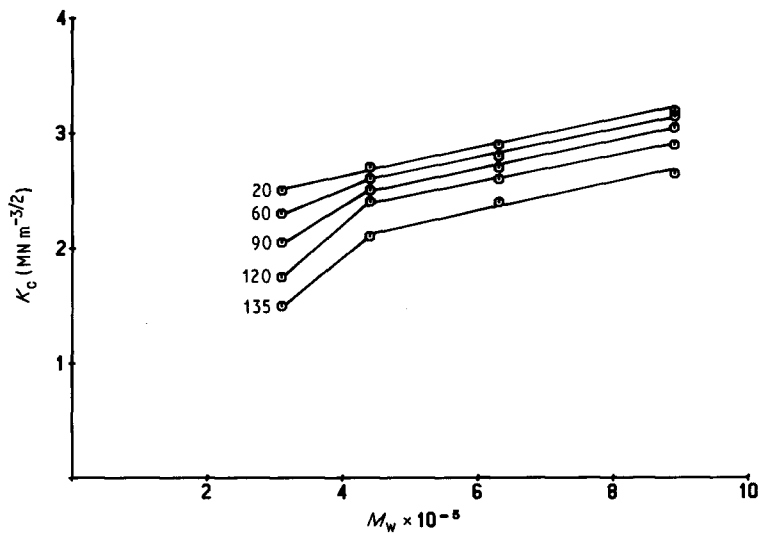


Figure 6 Critical stress intensity factor K_c as a function of molecular weight M_w , for unannealed PP samples crystallized at different temperatures T_b as indicated.

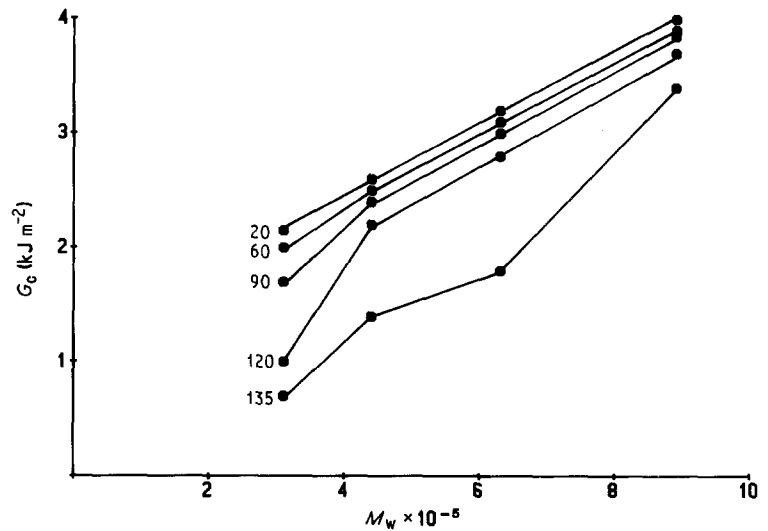


Figure 7 Critical strain energy release rate G_c as a function of molecular weight M_w , for annealed PP samples crystallized at different temperatures T_b as indicated.

fracture toughness is determined essentially by the energy required to strain and break the very few interspherulitic links, and hence low fracture parameter values are achieved.

Different features are observable on the fracture surface of the fine spherulitic material (Fig. 9b). In this case, in fact, a well-defined plastic zone ahead of the notch tip (see left side of the picture), with morphological characteristics similar to the mirror area of

the amorphous glassy polymers, is visible [15, 16]. The presence of such an island-type structure suggests that the onset of a crack is preceded by the formation of crazes. These crazes may develop and propagate within spherulites and interspherulitic regions because, due to the quenching treatment, the degree of interconnection in both areas is sufficiently high and hence the material is able to sustain large deformations before the final fracture occurs. Therefore the greater tough-

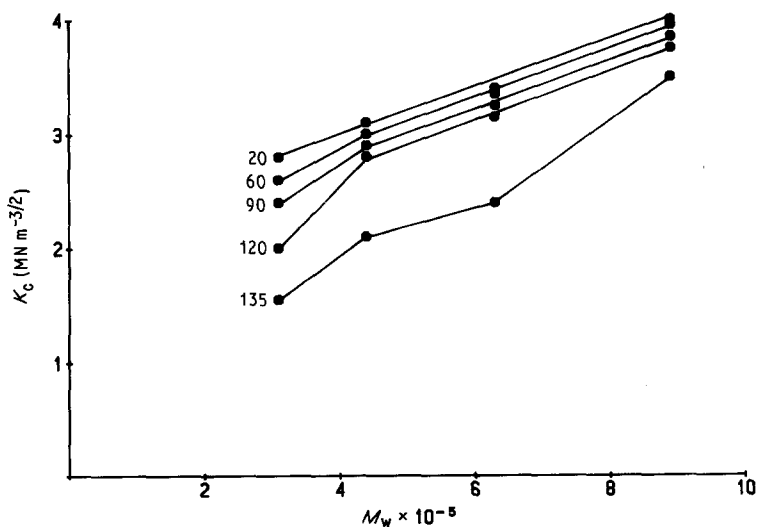


Figure 8 Critical stress intensity factor K_c as a function of molecular weight M_w , for annealed PP samples crystallized at different temperatures T_b as indicated.

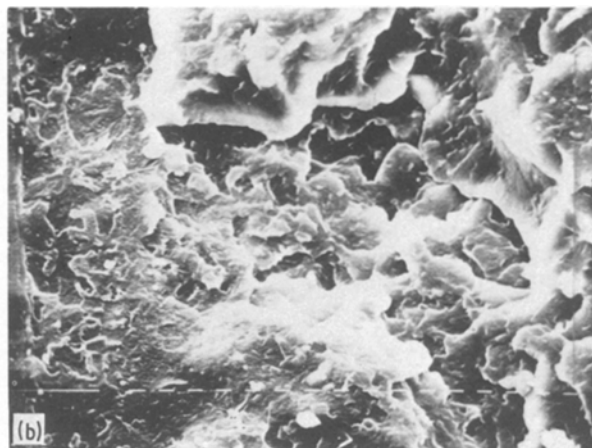
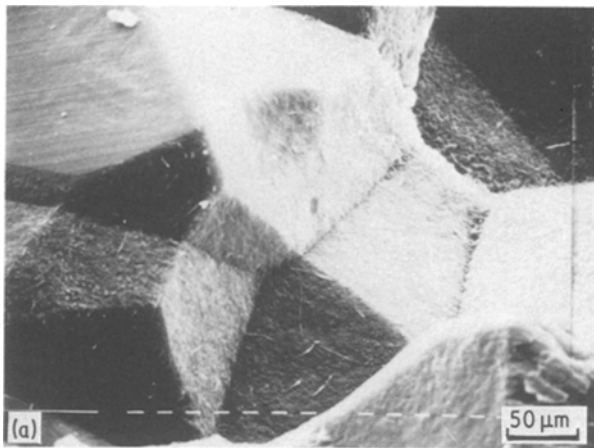


Figure 9 Scanning electron micrographs of fractured surfaces of unannealed PPI sample. (a) $T_b = 135^\circ\text{C}$, (b) $T_b = 20^\circ\text{C}$.

ness observed in the fine spherulitic sample arises from a larger energy dissipation due to the crazing mechanism. On the other hand, the amount of plastic deformation that can take place at the crack tip in both coarse and fine spherulitic morphologies can be strongly modified by changing the molecular weight. This is evident for coarse samples in Fig. 9a and 10. At increasing M_w , a higher degree of plastic deformation in the spherulitic boundary zones is observed as a consequence of the enhanced tendency to craze formation. Such a finding is due to the fact that with increasing M_w the interspherulitic link density, due to the better quality of the interlayered amorphous material, is enhanced (also in these regions such a

material has a higher M_w). On this basis the fracture will be controlled by the number and stability of the crazes formed ahead of the crack tip. The net effect is a strong improvement in the impact toughness with M_w .

A similar behaviour is observed for fine spherulitic materials. In fact, as shown in Fig. 9b and 11, the crazed area is greater the higher the molecular weight. Also this result can be associated with the fact that the interspherulitic and the intraspherulitic link density is highly improved by increasing M_w . Consequently numerous crazes with a very fine texture and a large resistance to breakdown can be formed in both regions. Thus a great hindrance to the crack propagation is achieved.

Further evidence that the fracture process is essentially controlled by the interconnections within the material (which in turn determine the craze structure) arises from the annealed specimens. Since annealing is believed to operate through a partial melting and recrystallization process in addition to lamellar thickening, the growth of thin crystallites into the amorphous zones and a rearrangement of uncrystallized polymer chains may occur. Therefore annealing should produce, especially for specimens crystallized at low T_b , a network that is physically more connected

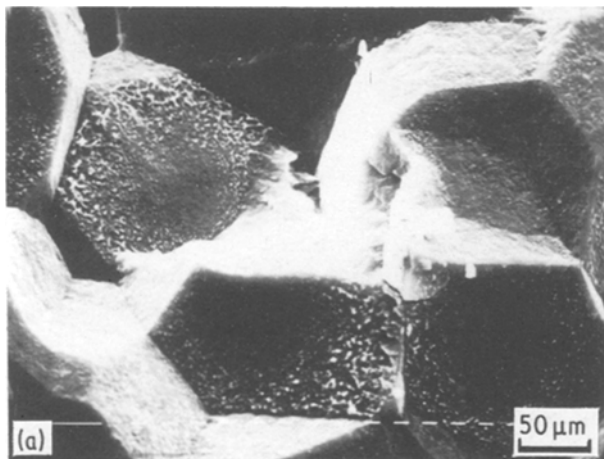
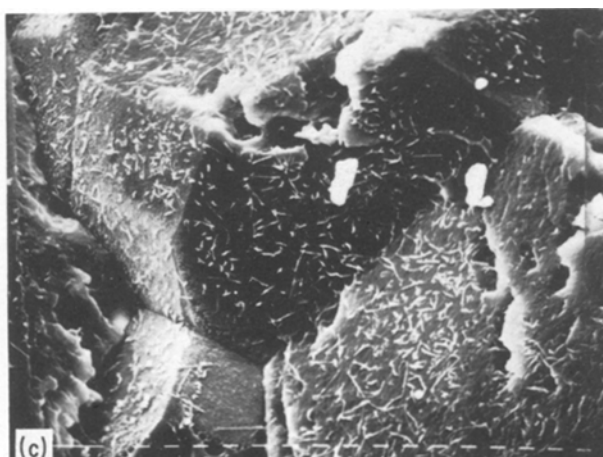


Figure 10 Scanning electron micrographs of fractured surfaces of unannealed PP samples of increasing molecular weight and $T_b = 135^\circ\text{C}$. (a) PP2, (b) PP3, (c) PP4.



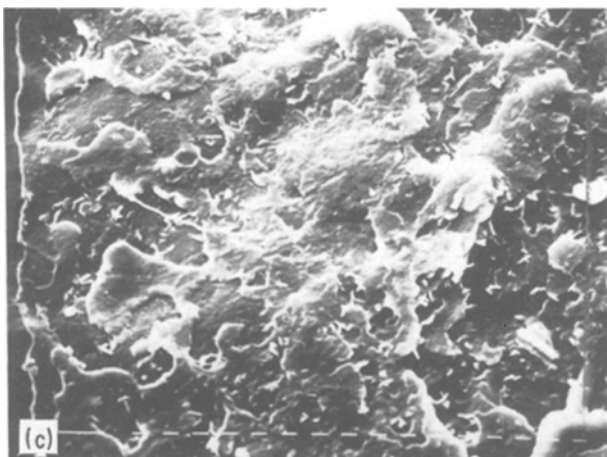
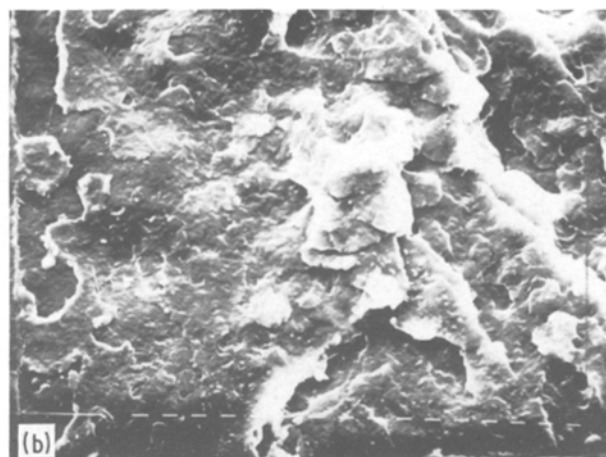
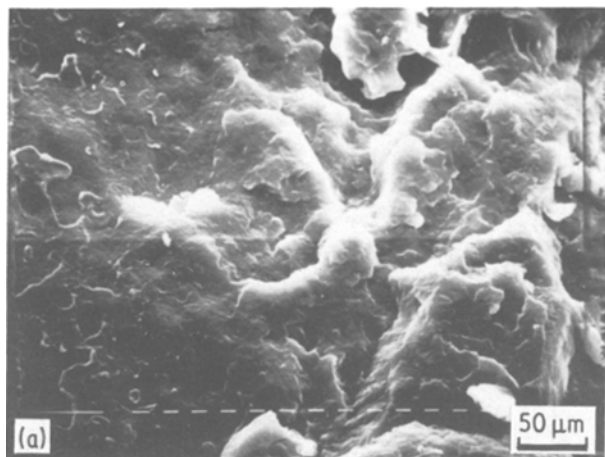


Figure 11 Scanning electron micrographs of fractured surfaces of unannealed PP samples of increasing molecular weight and $T_b = 20^\circ\text{C}$. (a) PP2, (b) PP3, (c) PP4.

than that of the corresponding unannealed samples. This makes possible a larger plastic deformation, due to the higher strength and stability of the crazed material. Such an effect is visible in Fig. 12, where the fracture surfaces of annealed fine spherulitic materials are reported. It can be seen that the area in which the crack initiates is greater relative to that of the unannealed specimens (compare Fig. 11 with Fig. 12), and it becomes more extended as M_w is increased. Furthermore for the highest M_w sample, highly elongated fibrils are visible in this area. The above points indicate that there is a notable enhancement in the work required for crack propagation in these materials according to the better fracture parameter values observed.

For samples crystallized at high T_b , as we have already reported, only for the highest M_w materials is the annealing procedure accompanied by a strong improvement in the impact fracture toughness. Also in this case an examination of the corresponding fracture surface (Fig. 13) shows evidence of extensive plastic deformations with a morphology (magnified in Fig. 13b) quite different from that of the unannealed sample (Fig. 10c). In other words, during annealing the zones which more easily undergo melting and recrystallization are probably the interspherulitic ones. Therefore the spherulites at the end are more tightly glued together. The comparison of such figures emphasizes again the role played by the structure of the spherulite boundaries in determining the craze texture and hence the impact fracture toughness.

Finally, the result that the annealing has little or no effect on the toughness of the lower M_w samples may be attributed to the fact that the samples are kept in the bath beyond the necessary crystallization times. In fact after complete crystallization the samples are annealed for several hours at 135°C (which is close to the annealing temperature of 140°C). This yields a very stable material and no further morphological changes can be obtained by the successive heat treatment. This has been confirmed by enhancing at $T_b = 135^\circ\text{C}$ the bath residence times. The values for each sample were calculated assuming that the relaxation time is proportional to M_w^3 [17]. As can be seen from Table IV, only for PP4 is there a change in the K_c and G_c values as a consequence of its more metastable state, whereas for PP2 and PP3 K_c and G_c are practically unchanged.

4. Conclusions

In this paper it has been shown that crystallization conditions, thermal treatment and molecular characteristics can strongly influence the structure, morphology and fracture impact toughness of isotactic polypropylene. In particular the following points can be made:

1. The amount of crystallinity and the melting point are lowered by decreasing T_b and by increasing M_w . These effects can be understood on the basis of the molecular mechanisms acting during the crystallization on polymers having different molar masses and molar mass distributions.

TABLE IV Fracture toughness parameters G_c and K_c for unannealed PP samples crystallized at $T_b = 135^\circ\text{C}$ with different residence times

Sample	T_b ($^\circ\text{C}$)	Time (h)	G_c (kJ m^{-2})	K_c ($\text{MN m}^{-3/2}$)
PP2	135	5	1.4	2.1
		17	1.3	2.0
PP3	135	5	1.8	2.4
		40	1.8	2.5
PP4	135	5	2.5	2.7
		135	3.4	3.5

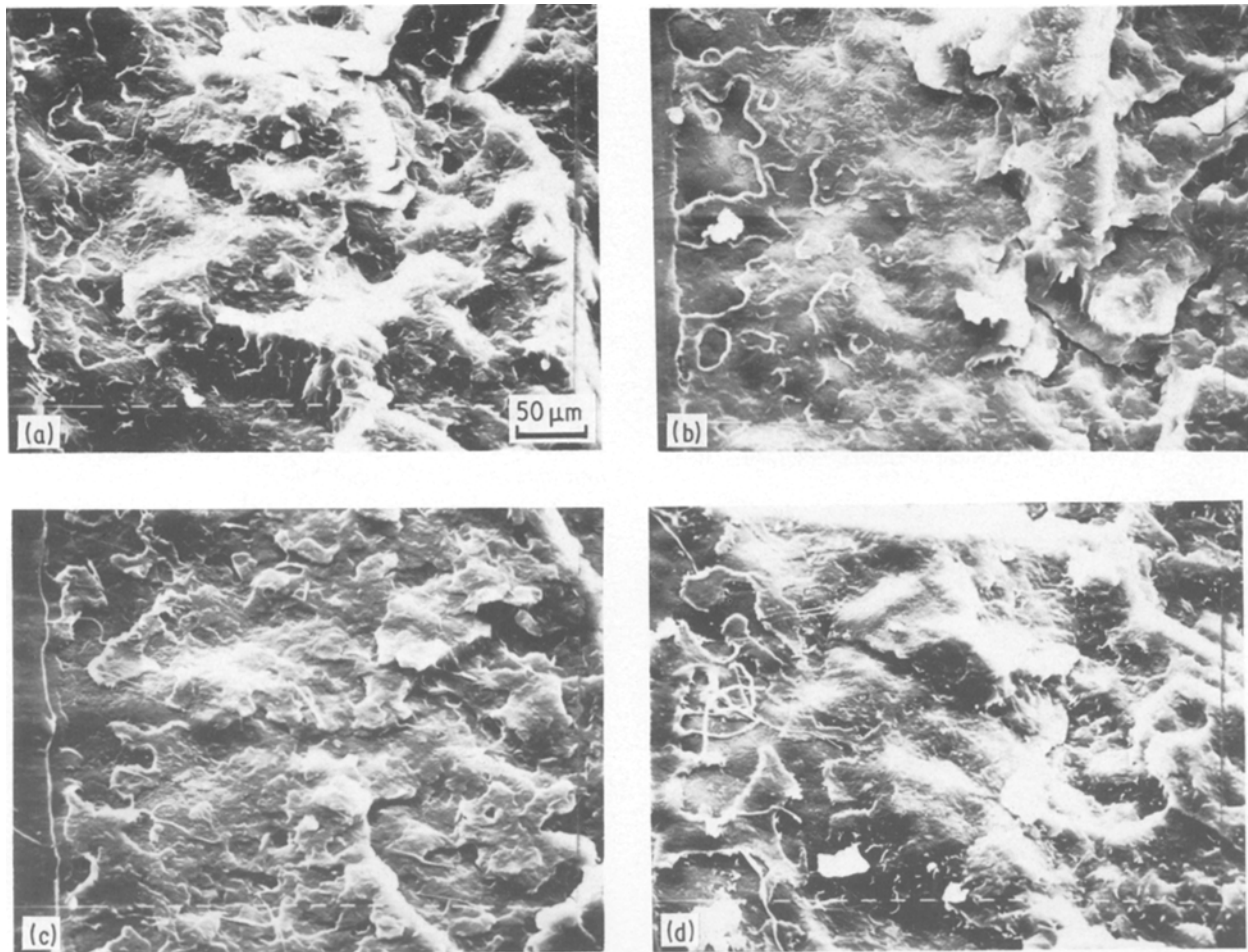


Figure 12 Scanning electron micrographs of fractured surfaces of annealed PP samples of increasing molecular weight and $T_b = 20^\circ\text{C}$. (a) PP1, (b) PP2, (c) PP3, (d) PP4.

2. A successive thermal treatment (annealing) increases X_c and has no influence on T_m . In the solidified samples the enhanced local molecular mobility induces new crystallization and molecular rearrangements.

3. The morphological architecture (lamellae, spherulites and interconnecting tie-molecules) is strongly affected by the above-mentioned molecular mechanisms.

4. Different molecular structures and superstructures determine in turn the overall properties. In fact G_c and K_c , which represent the resistance of the material prior to fracture, can be considered to be a

measure of the interconnection existing in the system. Since this structural network is built up during the crystallization and thermal treatment and depends on the molecular characteristics, G_c and K_c must depend on all the imposed conditions, as is the case. As a matter of fact they are so sensitive to them that can be used on the other hand as a useful tool for structural investigations.

Acknowledgement

The authors wish to express many thanks to Mr V. Di Liello and Mr M. Viola for their technical assistance.

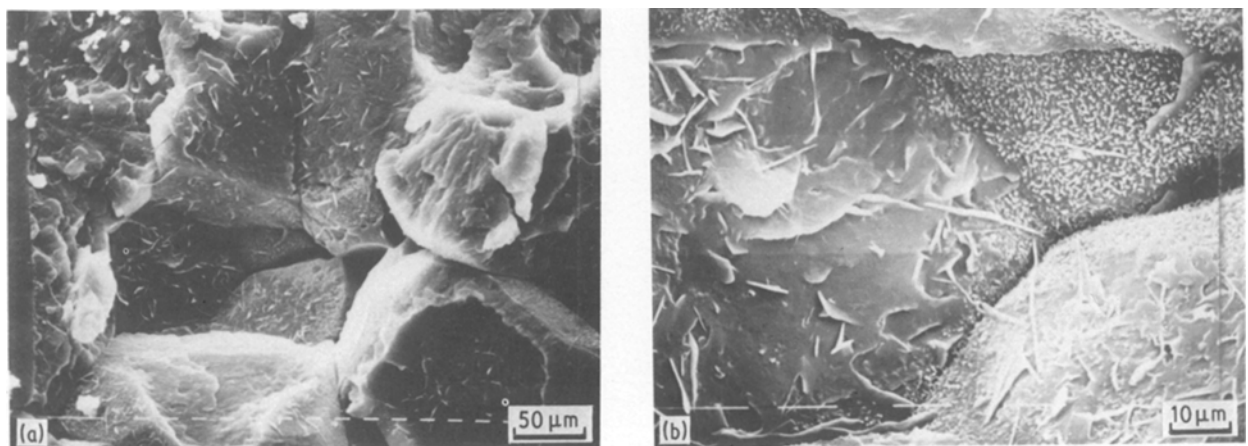


Figure 13 Scanning electron micrographs of fractured surfaces of annealed PP4 sample at $T_b = 135^\circ\text{C}$.

References

1. P. J. PHILLIPS and J. PATEL, *Polym. Eng. Sci.* **18** (1978) 93.
2. J. L. WAY, J. R. ATKINSON and J. NUTTING, *J. Mater. Sci.* **9** (1974) 293.
3. J. M. SCHULTZ, *Polym. Eng. Sci.* **24** (1984) 770.
4. M. J. McCREADY and J. M. SCULTZ, *J. Polym. Sci. Polym. Phys. Ed.* **17** (1979) 725.
5. K. FRIEDRICH, *Prog. Colloid. Polym. Sci.* **64** (1978) 103.
6. R. GRECO and F. COPPOLA, *Plast. Rubb. Process. Appl.* **6** (1986) 35.
7. J. H. REINSHAGEN and R. W. DUNLOP, *J. Appl. Polym. Sci.* **20** (1976) 9.
8. K. FRIEDRICH and U. A. KARSH, *J. Mater. Sci.* **16** (1981) 167.
9. B. Z. JANG, D. R. UHLMANN and J. B. van der SANDE, *Polym. Eng. Sci.* **25** (1985) 98.
10. H. H. KAUSCH, "Polymer Fracture" (Springer, Berlin, 1978).
11. A. LUSTIGER and R. L. MARKHAM, *Polymer* **24** (1983) 1647.
12. A. J. KINLOCH and R. J. YOUNG, "Fracture Behaviour of Polymers" (Applied Science, London, 1983).
13. W. F. BROWN and J. STRAWLEY, ASTM STP410 (American Society for Testing and Materials, Philadelphia, 1966) p. 13.
14. E. PLATI and J. G. WILLIAMS, *Polym. Eng. Sci.* **15** (1975) 470.
15. J. MURREY and J. HULL, *J. Polym. Sci. Part 2* **8** (1970) 583.
16. R. GRECO and G. RAGOSTA, *Plast. Rubb. Processg Appl.* **7** (1987) 163.
17. J. D. FERRY, "Viscoelastic Properties of Polymers," 3rd Edn (Wiley, New York, 1980) p. 251.

*Received 27 July
and accepted 23 October 1987*